Supporting information:

Title: $LiIn_2SbO_6$: A New Rutile-Related Structure-type with Unique Ion Channels

Authors: Steven Flynn[1], Sheel Sanghvi[2], Matthew L. Nisbet[1], Kent J. Griffith[1], Weiguo Zhang[3], P. Shiv Halasyamani[3], Sossina M. Haile[1,2], Kenneth R. Poeppelmeier[1]

[1] Department of Chemistry, Northwestern University, Evanston, Illinois 60208, United States
[2] Department of Materials Science and Engineering, Northwestern University, Evanston, Illinois 60208, United States
[3] Department of Chemistry, University of Houston, Houston, Texas, 77204, United States

E-mail: krp@northwestern.edu

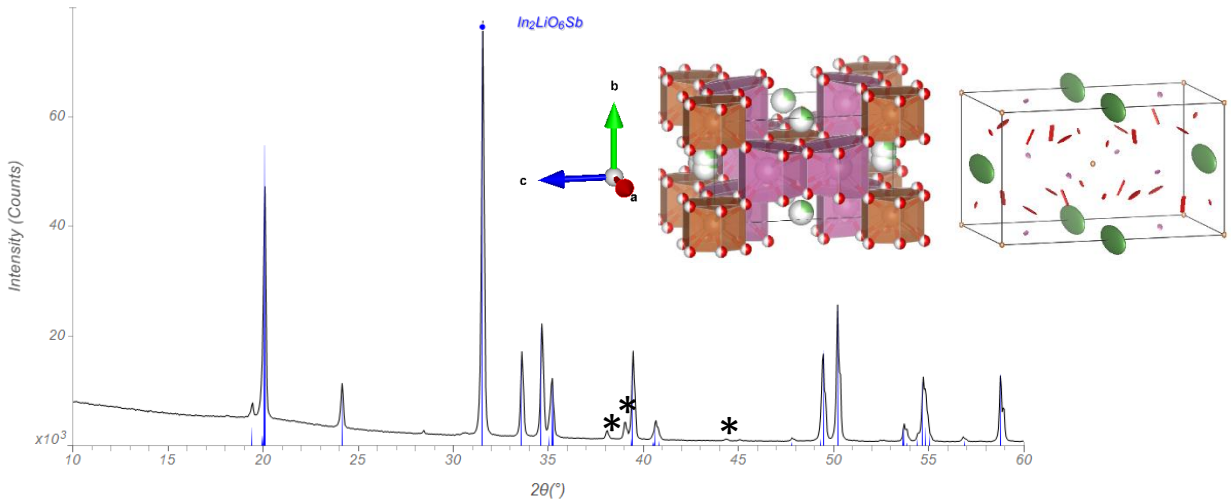

Figure S1: Body-centered crystal structure solutions of $LiIn_2SbO_6$ and their predicted PXRD patterns compared with the experimentally observed one. Only one predicted pattern is shown for simplicity, as the two are visibly identical. Peaks marked with an asterisk are unaccounted for by the body-centered structures but present with the primitive solution presented in the main text, indicating the qualitatively better fit of the latter. The left (*Immm*) structure demonstrates that each layer of half-filled O positions consists of two individual orientations of a close-packed layer super imposed on top of each other. The right structure (*I222*) shows the unrealistically flat or non-positive definite (cylinders) ellipsoids apparent in some 100 K body-centered solutions.

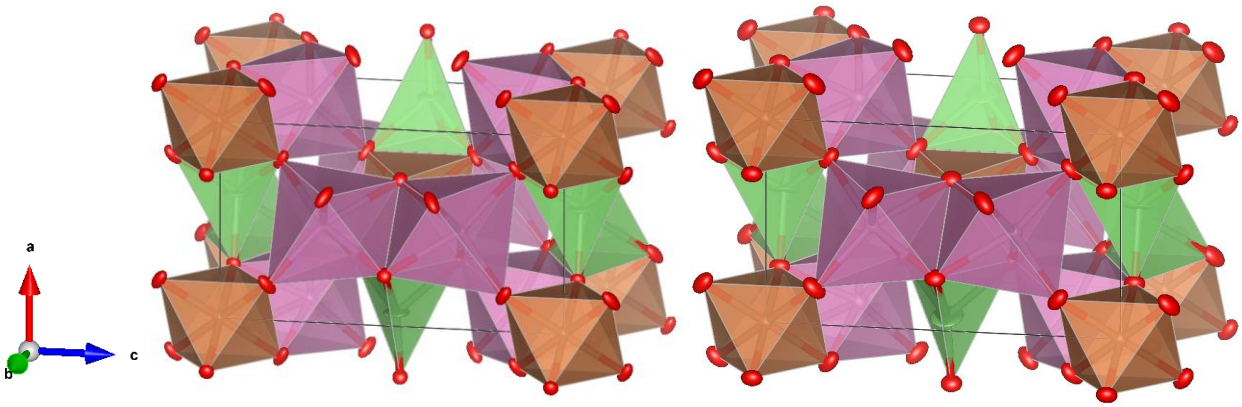

Figure S2: Single crystal structural solutions for LIAO at 323 (left) and 500 K (right). The structures are overall the same as each other and the 100 K structure presented in the main text, with increasing atomic displacement parameters at higher temperatures.

Table S1: Rietveld Refinement parameters

Source	Laboratory X-ray
Chemical Formula	$LiIn_2SbO_6$
Formula Weight	454.33
Temperature (K)	298
Wavelength (Å)	1.54 (CuKα)
Crystal System	Orthorhombic
Space group (No.)	Pnnm (58)
a (Å)	5.10174(4)
b (Å)	5.33510(4)
c (Å)	8.88091(6)
α = β = γ (deg)	90
V ($Å^3$)	241.723(3)
Z	2
Profile range	$10 \leq 2\Theta \leq 120$
GOF	2.65
R_p (%)	6.22
R_{wp} (%)	8.88

Table S2: Atomic coordinates in LIAO at 323 and 500 K.

Atom	Wyckoff Position	x	y	z	U_{eq}*
323 K					
In	4f	0.5	0	0.30041(2)	6.05(9)
Sb	2a	0.5	0.5	0.5	5.23(9)
Li	4g	0.046(3)	0.101(3)	0.5	24(3)
O1	8h	0.2787(3)	0.3364(3)	0.34378(13)	11.7(3)
O2	4g	0.6980(4)	0.1842(3)	0.5	7.2(3)
500 K					
In	4f	0.5	0	0.29965(4)	9.4(2)
Sb	2a	0.5	0.5	0.5	7.4(2)
Li	4g	0.049(4)	0.086(5)	0.5	29(6)
O1	8h	0.2801(5)	0.3362(6)	0.3432(3)	15.5(6)
O2	4g	0.6979(6)	0.1843(7)	0.5	12.6(7)

*For full anisotropic displacement parameters, see CIFs.

Table S3: Selected M-O bond-lengths, O-M-O bond angles, and Multiplicities in LIAO (323 and 500 K)

bond lengths (Å)		angles (°)	
323 K			
2x In-O1	2.1533(16)	1x O1-In-O1	105.00(6)
2x In-O1	2.1012(14)	2x O1-In-O1	96.59(6)
2x In-O2	2.2628(12)	2x O1-In-O1	95.76(6)
		2x O1-In-O2	89.70(4)
		2x O1-In-O2	89.29(3)
		1x O2-In-O2	76.98(1)
		2x O1-In-O2	74.49(3)
4x Sb-O1	1.9888(14)	4x O2-Sb-O1	94.83(5)
2x Sb-O2	1.9627(17)	2x O1-Sb-O1	91.63(5)
		2x O1-Sb-O1	88.37(5)
		4x O2-Sb-O1	85.18(5)
2x Li-O1	2.214(12)	1x O2-Li-O2	142.7(9)
1x Li-O2	1.829(16)	2x O2-Li-O1	112.49(4)
1x Li-O2	2.004(16)	2x O2-Li-O1	94.63(4)
		1x O1-Li-O1	77.51(5)
500K			
2x In-O1	2.152(2)	1x O1-In-O1	105.85(10)
2x In-O1	2.104(3)	2x O1-In-O1	96.81(11)
2x In-O2	2.271(2)	2x O1-In-O1	95.63(11)
		2x O1-In-O2	89.36(7)
		2x O1-In-O2	89.24(7)
		1x O2-In-O2	76.85(1)
		2x O1-In-O2	74.44(8)
4x Sb-O1	1.992(3)	4x O2-Sb-O1	94.86(9)
2x Sb-O2	1.965(4)	2x O1-Sb-O1	91.31(11)
		2x O1-Sb-O1	88.69(11)
		4x O2-Sb-O1	85.14(9)
2x Li-O1	2.262(19)	1x O2-Li-O2	148.2(12)
1x Li-O2	1.87(2)	2x O2-Li-O1	109.67(7)
1x Li-O2	1.93(2)	2x O2-Li-O1	95.13(7)
		1x O1-Li-O1	77.97(10)

Table S4: Bond Valence Analysis in LIAO at 100 K

Site	In^{3+}	Sb^{5+}	Li^{+}
2a	4.83	**5.00**	1.49
4f	**2.94**	3.26	0.91
4g	2.86	2.98	**0.88**

*BVS values calculated for all three cations at each site. Bold Values indicate the best match between Bond Valence and expected charge of a species at each cation site.

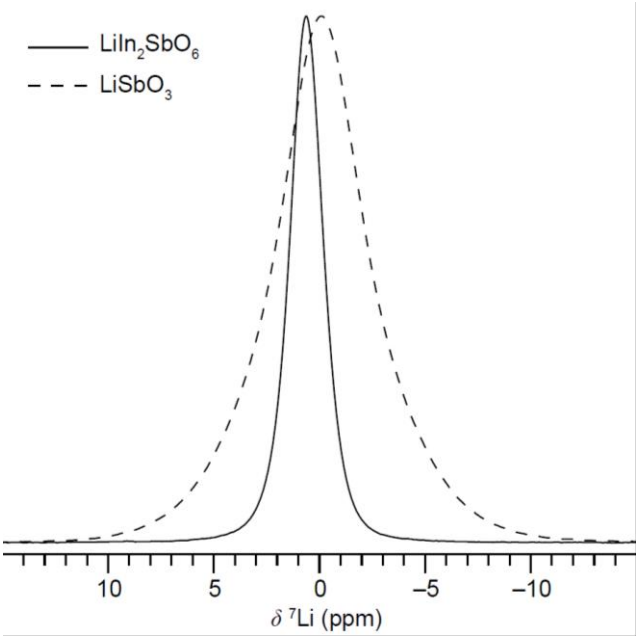

Figure S3: ^{7}Li NMR spectra of the central resonance of LIAO and LiSbO3. Note the increased linewidth vs. 6Li and the difference in *x*-axis scale compared to **Figure 3**. ^{6}Li provides narrower lines than ^{7}Li due to its smaller dipolar and quadrupolar broadening. Spinning at 12.5 kHz showed no line narrowing of the central transition relative to 5 kHz. Furthermore, the full-width half-maximum linewidths of $^{6}LiIn_2SbO_6$, $^{7}LiIn_2SbO_6$, $^{6}LiSbO_3$, $^{7}LiSbO_3$ are 50, 280, 95, and 750 Hz. Dipolar coupling scales according to $D_{jk} = \gamma_j \gamma_k \left(\frac{h}{4\pi^2}\right)\left(\frac{\mu_0}{4\pi}\right) r_{jk}^{-3}$, where $\gamma_{j,k}$ are the gyromagnetic ratios of isotope *j* and *k*, respectively, and r_{jk} is the distance between isotopes *j* and *k*. Thus homonuclear dipolar coupling has a γ^2 dependence and the expected difference between ^{6}Li (γ= 6.2655 MHz/T) and ^{7}Li (γ= 16.5471 MHz/T) is approximately a factor of 6.97. These differences between lithium nuclei, and the increased linewidth in $LiSbO_3$ with face-sharing Li octahedra versus $LiIn_2SbO_6$ with isolated lithium tetrahedra, are consistent with MAS line broadening dominated by noncommuting homonuclear Li–Li dipolar couplings.

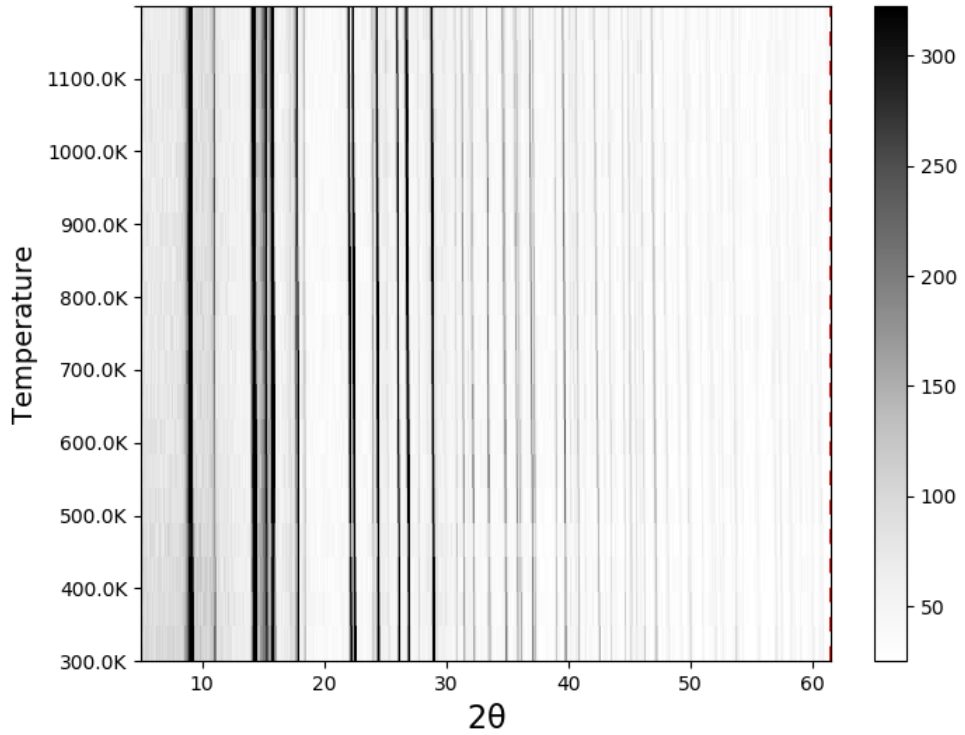

Figure S4: Temperature-dependent PXRD pattern of LIAO from 300 to 1200 K.

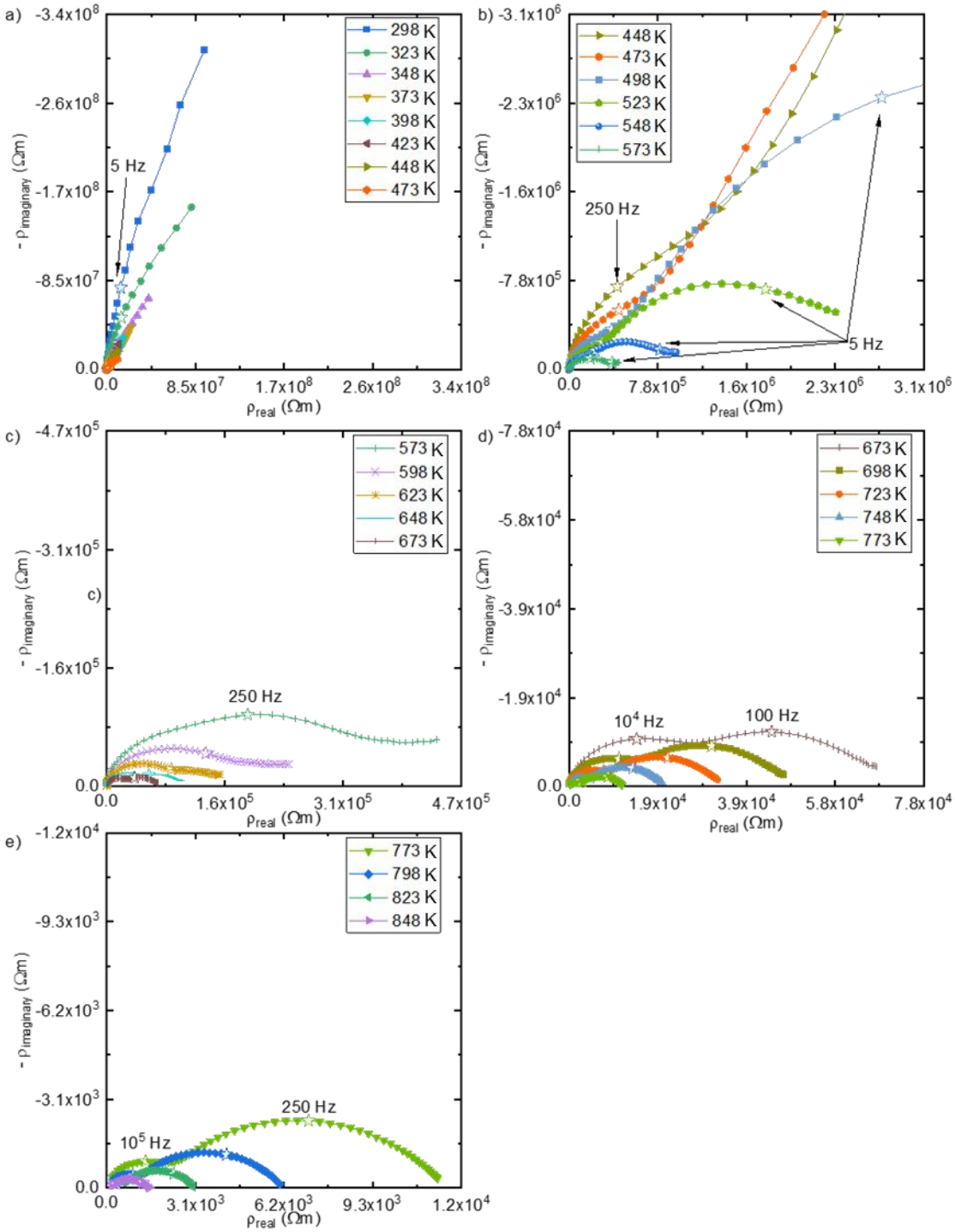

Figure S5: Temperature-dependent impedance spectra of LIAO from: (a) 298 to 473 K, (b) 448 to 573 K , (c) 573 to 673 K, (d) 673 to 773 K, and (e) 773 to 848 K. Spectra are measured under synthetic air. Select frequencies are indicated by a star.

References:

1. David C. Apperley, Robin K. Harris, Paul Hodgkinson. *Solid-State NMR: Basic Principles and Practice*. Momentum Press, New York, **2012.**